

CALCULATING TRUE STRATIGRAPHIC AND TRUE VERTICAL THICKNESS

©2012 by Charles R. Berg

ABSTRACT

Methods for calculating true stratigraphic thickness (*TST*) and true vertical thickness (*TVT*) traditionally have assumed no borehole curvature and constant dip. In order to account for borehole curvature, best practice is suggested in which coordinates calculated from borehole deviation surveys are used directly in the calculations. In order to account for changing dip, three new, fully 3-dimensional (3D) vectoral methods are developed. Other recommended best practices involve proper methods of dip and deviation averaging and interpolation.

INTRODUCTION

Standard practice for calculating true stratigraphic thickness (*TST*) and true vertical thickness (*TVT*) involves a single dip, a single deviation measurement and a measured-depth interval (Figure 1). The usual procedure is to plug in dip, dip azimuth, borehole inclination, and borehole azimuth at the top of a bed, along with the measured depth interval, into a standard equation (for example, Tearpock and Bischke, 1991).

Since dip and deviation both are usually different at the top and bottom of a given interval, how are the calculations adjusted accordingly? The deviation issue will be resolved by first putting the problem into vectoral form and using spatial coordinates derived from deviation calculation. In essence, the derivations of *TVT* and *TST* equations assume a straight line, and the borehole deviation coordinates provide just that.

To solve the two-dip problem, three solutions are developed. The simplest, vector averaging, which assumes that the change in dip is caused by random error, calculates an averaged dip to substitute into the vectoral formula. The other two methods are based on two different geometric assumptions. The first, the fold-vector method,

assumes that the change in dip is caused by concentric folding. The second, the wedge-vector method, assumes that the change in dip is caused by stratigraphic thinning or thickening.

TVT is the vertical distance from the point where the borehole intersects top of the bed to the base of the bed. This distance depends directly on the bed thickness (or *TST*). Therefore, *TST* will mainly be discussed here. However, methods for calculating *TVT* will be given for the new *TST* models.

Two recent papers have introduced two-dip models for calculating *TST*, Xu, et al. (2007) and Xu, et al. (2010). Both papers implicitly assume that the upper and lower dips have the same azimuth. Therefore, they are not fully 3D methods, although they were adapted here as 3D methods in order to check the calculations on the fold-vector and wedge-vector models (see Appendix).

METHODS

Single-Dip Equations

The Setchell Equation

Following is the formula for *TST* from Tearpock and Bischke (1991):

$$TST = MT (\cos \psi - \sin \psi \cos(\theta_d - \theta_b) \tan \phi) \cos \phi, \quad (1)$$

where *MT* = measured thickness, *TST* = true stratigraphic thickness, ϕ = dip, θ_d = the dip azimuth, ψ = borehole inclination, and θ_b = borehole azimuth. Equation 1 is commonly referred to as the ‘‘Setchell’’ equation. To calculate *TVT*, *TST* is divided by the cosine of the dip or

$$TVT = \frac{TST}{\cos \phi}. \quad (2)$$

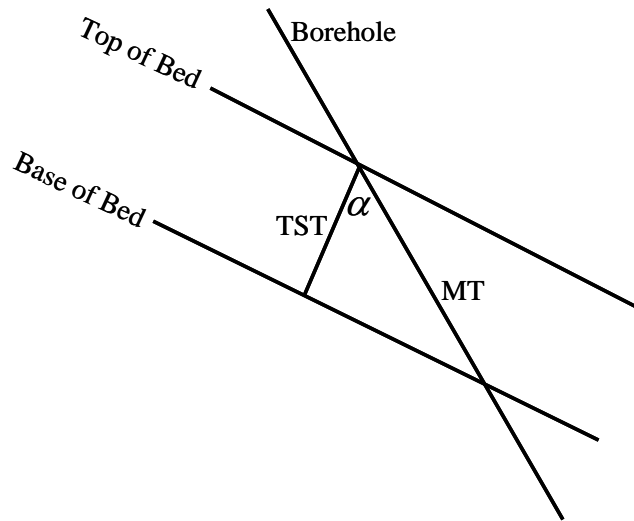


Figure 1. Diagram showing the configuration of the borehole and a bed whose *TST* is being calculated. *MT* is the difference in measured depth. The plane of section does not have to be vertical, but the borehole and the dip normal do have to lie within it. This is a fully three-dimensional (3D) technique.

Equation 1 is probably the most widely used equation for calculation of *TST* and *TVT*, but several other published equations produce identical results, among them are Holt, et al., 1977, and Marshak and Mitra, 1988.

The Vectoral Single-Dip Equation

Figure 2 shows Figure 1 in vectoral form. The vector **D** is the lower hemisphere pole of the dip and has a length of *TST*. The vector **B** has the spatial coordinates of the borehole deviation and has a length of *MT*. The angle α is the angle between the two vectors. From Figure 2 it can be seen that

$$TST = MT \cdot \cos \alpha . \tag{3}$$

This equation was published in Bateman and Hepp (1981). Although they did not explicitly state that they were using a vectoral method, from context it is likely they did. Since the cosine of the angle between two vectors is the dot product, equation 3 in vectoral notation is

$$TST = MT \cdot \hat{D} \cdot \hat{B}, \quad (4)$$

where \hat{D} is the lower-hemisphere dip-pole direction and \hat{B} is the borehole direction. (The “hat” notation on the vectors denotes unit vectors.)

Spherical to rectangular conversion routines for calculating dip and deviation vectors are listed in the Appendix in equations A-1 to A-6. Other coordinate systems may be used as long as dips and deviations are consistent with each other, that is, dips and deviations are lower-hemisphere poles.

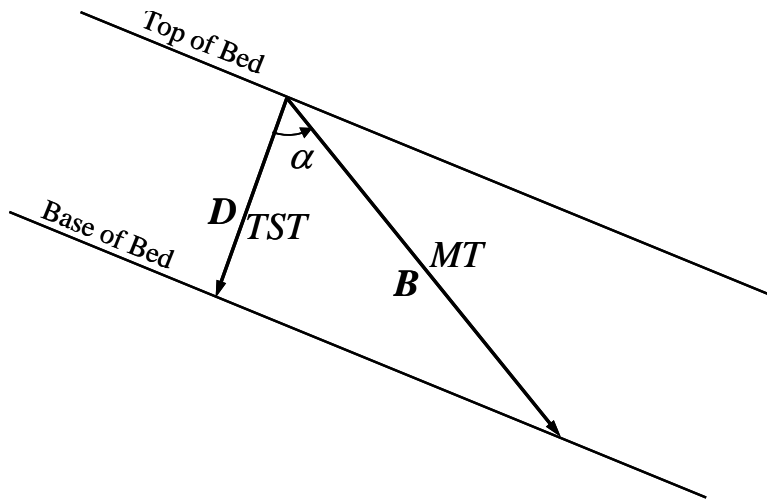


Figure 2. Figure 1 in a vectoral configuration. As with the lines TST and MT in Figure 1, vectors D and B both lie within the same plane, but that plane is not necessarily vertical.

Since the borehole vector B is equal to $MT \cdot \hat{B}$, equation 4 can be written

$$TST = \hat{D} \cdot B. \quad (5)$$

In terms of the vector components, equation 5 is

$$TST = \hat{D}_x B_x + \hat{D}_y B_y + \hat{D}_z B_z. \quad (6)$$

Equations 5 and 6 are different forms of the vectoral single-dip equation. Combining equations 2 and 3, the vectoral equation for TVT is

$$TVT = \frac{TST}{-\hat{D}_z}. \quad (7)$$

Although there is no published derivation for the Setchell equation (1), it can be derived directly from the vectoral single-dip equation 4. Formulas for spherical to rectangular coordinate conversion can be substituted into equation 6 to produce equation 1 (see Appendix).

Using Deviation Measurements

It is assumed here that the deviation calculation that is being done is based on the minimum curvature method (Taylor and Mason, 1972). Even if that is not the case, any good deviation calculation method should be able to provide rectangular coordinates suitable for calculation of *TST*. However, calculation methods that use techniques such as spline fits may not be amenable to interpolation techniques discussed below unless they have corresponding methods of interpolation.

Equation 6 automatically honors both top and bottom deviations, because both are used in the calculation of the deviation coordinates. In addition, the straight-line distance *MT* is used implicitly, as opposed to traditional methodology which simply uses the difference in measured depth. Of course, it is possible to use the Setchell equation (1) in the same way by converting the borehole vector to spherical coordinates, but it is simpler to use equation 6.

Figure 3 shows a borehole superimposed over the vectors shown in Figure 2. It is clear that the difference in measured depth will be larger than the straight-line distance *MT*. Although significant, the error caused by using measured depth can be small compared to the error caused by using only one of the deviation measurements.

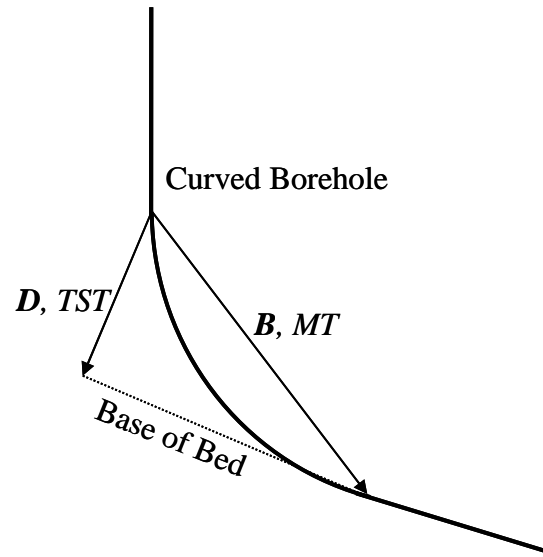


Figure 3. The same configuration in Figure 2 but with a highly deviated borehole. In this example it is clear that simply taking the difference in measured depth of the bottom and top of the bed will not give the correct length for *MT* and therefore *TST*. Furthermore, using either deviation by itself is totally inadequate for calculating *TST*, since the end-point deviation values differ a great deal from the overall deviation.

Using Figure 3 for an approximate configuration, assume that everything is in the same vertical plane of section. Using a measured-depth interval of 500m, dip of 23°, top inclination of 0°, and bottom inclination of 73°, *MT* calculates at 467m. Using that value for *MT* results in *TST* of 237m, while the result from using measured depth is 254m. Furthermore, if the calculation uses only the top deviation, as is customary, calculated *TST* is 460m, nearly twice the actual value. Most surprising, if only the lower deviation value is used, the *TST* comes out to -52m, which initially seems to be calculated wrong. It is not wrong, however, because the borehole in such a configuration would actually be traveling slightly up section and *TST* is negative when the borehole is traveling up section, and the calculation using the lower deviation has, in effect, projected that

deviation all the way up the borehole. See the section on the sign of *TST* for a detailed explanation on its significance.

Three New Two-Dip Models

The Average-Vector Method

The average-vector method expands on the vectoral single-dip equation by replacing the single dip vector with a vector representing the average of the upper and lower dips. Figure 4 shows the configuration of the average-vector method for finding *TST*. The simplest way to calculate the vector average \hat{D} is to normalize the vector sum:

$$\hat{D} = \frac{\hat{D}_1 + \hat{D}_2}{|\hat{D}_1 + \hat{D}_2|}, \quad (8)$$

where \hat{D}_1 and \hat{D}_2 are the dip vectors (lower hemisphere poles to dip.) *TST* is calculated by substituting \hat{D} from equation 8 into equation 5.

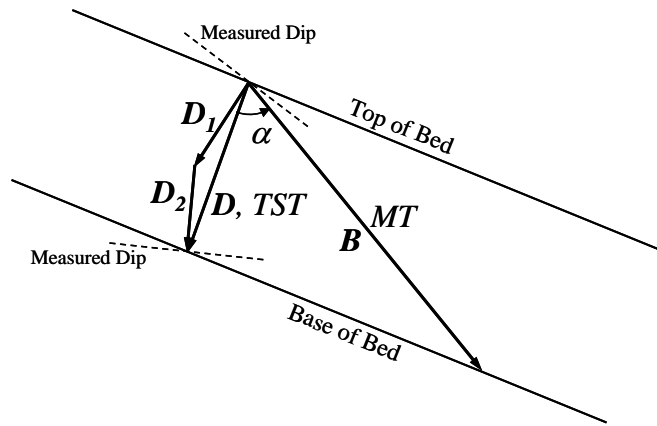


Figure 4. The average-vector method for incorporating both top and bottom dips. Since only the direction \hat{D} is needed in equation 5, it can be found as the normalized sum of the two measured-dip poles \hat{D}_1 and \hat{D}_2 .

The average-vector method is fully 3D. Strictly speaking, however, it is an approximation because it does not have an underlying geometric basis. In other words, the actual top and base of the bed in Figure 4 should somehow be related physically to

vectors D and B . This method was developed for use with borehole-imager derived dips where random scatter caused by both measurement error and random variation is present in the original data. Of the two-dip methods derived here, this one is by far the most efficient.

The conversion to TVT for the average-vector method uses equation 7, except that the z component is from the average vector \hat{D} .

The Fold-Vector Method

The derivation of the fold-vector equation assumes that concentric folding causes the difference in dip and that the stratigraphic thickness is constant. The top and bottom beds are defined by circular arcs, the end points of which are connected by vectors whose lengths are TST and whose directions are the dip poles (Figure 5).

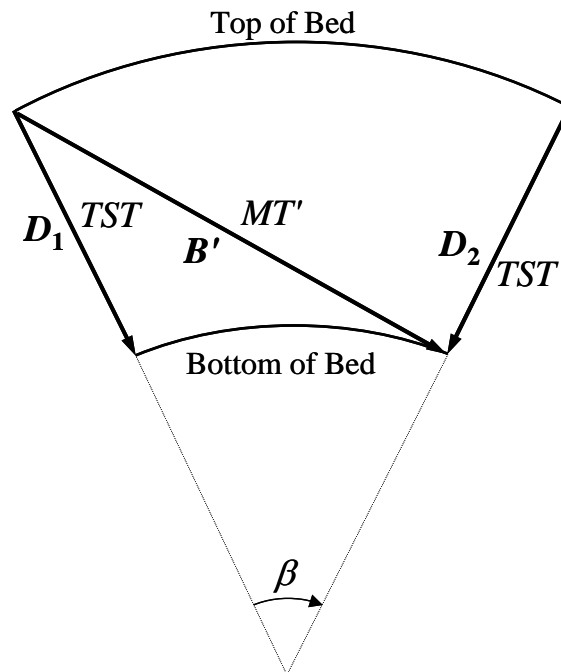


Figure 5. The fold-vector configuration with concentric arcs for the top and bottom of the bed, terminated by the vectors D_1 and D_2 representing vectors whose lengths are TST and whose directions are the top and bottom poles to dip. As in the previous figures, the vectors lie in the same plane, but not necessarily a vertical one.

In the average-vector derivation above, the model is set up within the plane created by the borehole and the average-dip vector. In contrast, the fold-vector derivation as well as the wedge-vector derivation below the models are set up in the plane formed by the two dip poles. In order to derive the relationships, the borehole first has to be projected onto the plane in which the two dip vectors lie. Below is the formula for projecting the borehole onto the two-dip plane:

$$\mathbf{B}' = \mathbf{B} - \hat{\mathbf{N}} \times (\hat{\mathbf{N}} \cdot \mathbf{B}), \quad (9)$$

where $\hat{\mathbf{N}}$ is the normal to the two-dip plane. (See the Appendix for the derivation.)

Figure 6 shows the angular relationships used in the derivation. Using the law of sines we get

$$TST = MT' \cdot \frac{\sin(\lambda)}{\sin(\delta)}, \quad (10)$$

where MT' is the length of $\bar{\mathbf{B}}'$. Since $\delta = \pi/2 - \beta/2$, equation 10 simplifies to

$$TST = MT' \cdot \frac{\sin(\gamma)}{\cos\left(\frac{\beta}{2}\right)}, \quad (11)$$

the fold-vector equation. The angle γ can be found as the arc cosine of the dot product of vectors $\hat{\mathbf{C}}$ and $\hat{\mathbf{B}}'$:

$$\gamma = \cos^{-1}(\hat{\mathbf{C}} \cdot \hat{\mathbf{B}}'), \quad (12)$$

where the vector $\hat{\mathbf{C}}$ is calculated as the normalized difference of the two dip vectors:

$$\hat{\mathbf{C}} = \frac{\hat{\mathbf{D}}_1 - \hat{\mathbf{D}}_2}{|\hat{\mathbf{D}}_1 - \hat{\mathbf{D}}_2|}. \quad (13)$$

The angle β can be found as the arccosine of the dot product of the two dip vectors:

$$\beta = \cos^{-1}(\hat{\mathbf{D}}_1 \cdot \hat{\mathbf{D}}_2). \quad (14)$$

Equations 11 through 14 constitute the fold-vector method.

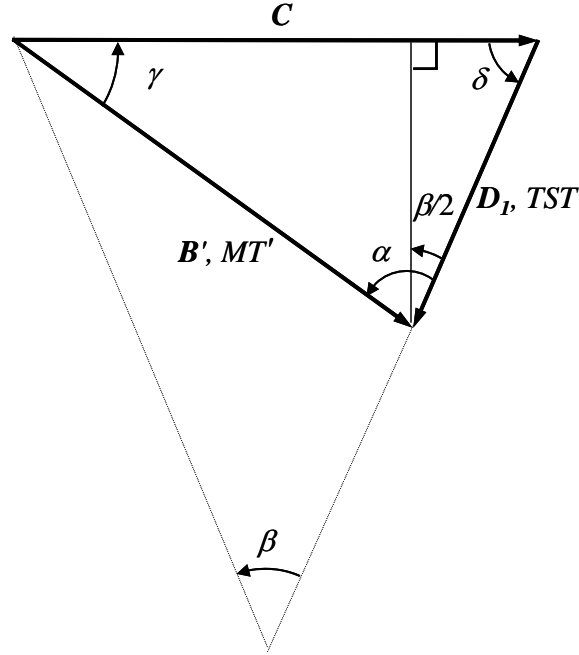


Figure 6. The angular relationships used in the derivation of the fold-vector method. Note that angle β is the angle between the two dip vectors D_1 and D_2 (see Figure 5).

The configuration of the fold-vector model makes calculating TVT complicated. The reason is that the TVT should be calculated as the length of a vertical line which passes through the top surface and intersects the base surface of the folded bed. The derivation involves the intersection of a vertical line with the cylindrical surface representing the base-bed boundary (see Appendix for derivation). Following are the equations, in calculation order, for finding fold-vector TVT :

$$R = \frac{TST \sin \alpha}{2 \sin \gamma \sin \left(\frac{\beta}{2} \right)}, \quad (15)$$

$$E = D_1 (\pm R - TST), \quad (16)$$

$$F = \hat{N}_x E_y - \hat{N}_y E_x, \quad (17)$$

$$G = \hat{N}_x E_z - \hat{N}_z E_x, \quad (18)$$

$$H = \hat{N}_y E_z - \hat{N}_z E_y, \quad (19)$$

$$A = \hat{N}_x^2 + \hat{N}_y^2, \quad (20)$$

$$B = \hat{N}_x G + \hat{N}_y H, \quad (21)$$

$$C = F^2 + G^2 + H^2 - R^2, \text{ and} \quad (22)$$

$$TVT = -\frac{B \pm \sqrt{B^2 - A \cdot C}}{A}, \quad (23)$$

where R is the radius of the base-bed cylinder and E is the distance of the cylindrical axis from the origin.

The Wedge-Vector Method

The wedge-vector derivation assumes that TST is measured perpendicular from the top of the bed (Figure 7). From the law of sines,

$$TST = MT' \frac{\sin \gamma}{\sin \delta}. \quad (24)$$

From the relationship of the angle sum of a triangle,

$$\delta = \frac{\pi}{2} - \beta \text{ and} \quad (25)$$

$$\gamma = \pi - \alpha - \delta. \quad (26)$$

Substituting equation 25 into equation 26 gives γ in terms of α and β :

$$\lambda = \frac{\pi}{2} - (\alpha - \beta). \quad (27)$$

Substituting equations 25 and 27 into equation 24 and simplifying yields

$$TST = MT' \frac{\cos(\alpha - \beta)}{\cos(\beta)}. \quad (28)$$

In the case where the bed is thinning to the left, $\cos(\alpha - \beta)$ in equation 28 becomes $\cos(\alpha + \beta)$. Finding the correct sign for β will be discussed more fully below. The angle β itself, which is the angular difference between the beds, can be found using equation 14. To find α , we use the dot-product relationship for the angle between two vectors:

$$\alpha = \cos^{-1} \left(\frac{\hat{D}_1 \cdot B'}{MT'} \right). \quad (29)$$

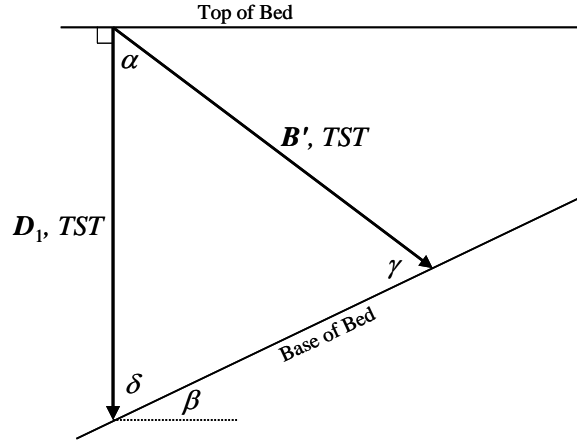


Figure 7. The wedge-vector configuration. As in the fold-vector figures, the vectors lie within the same plane, but not necessarily a vertical one. The angle β is the angular difference between the two dip planes, which is the same as the angle between the two dip poles.

As in the fold-vector method, the vector \mathbf{B}' and its length MT' can be found by projecting parallel to the intersection of the top and base of the wedge, which happens to be mathematically identical to a fold axis calculated using the same beds. In other words, the vector \mathbf{B}' can be calculated using equation 9.

Perhaps the most challenging part of the wedge-vector method is finding the sign of β in equation 28. Figure 7 is in a non-vertical plane in which the relative sense of the thinning cannot be determined simply on the angular relationships. In other words, terms such as “up”, “down”, “right” and “left” are only relative to the figure in that plane.

Mathematically, it is desirable to find a relationship that can determine relative orientation. One way to find left-thinning versus right-thinning is to determine the measurement directions of $\hat{\mathbf{D}}_1$ to $\hat{\mathbf{D}}_2$ with the direction of $\hat{\mathbf{D}}_1$ to $\hat{\mathbf{B}}'$. This is done by the relationship

$$s = (\hat{\mathbf{D}}_1 \times \hat{\mathbf{D}}_2') \cdot (\hat{\mathbf{D}}_1 \times \hat{\mathbf{B}}'), \text{ or} \quad (30)$$

$$s = \hat{\mathbf{N}} \cdot (\hat{\mathbf{D}}_1 \times \hat{\mathbf{B}}'). \quad (31)$$

($\hat{\mathbf{N}}$ should already be calculated when finding TST using equation A-9.) If

s is positive, the angles are measured the same direction and the bed is thinning right, if s is negative, the angles are measured opposite directions and the bed is thinning left.

Inserting s into equation 28 yields

$$TST = MT \cdot \frac{\cos(\alpha - s \cdot \beta)}{\cos(\beta)}. \quad (32)$$

Equation 32 along with equations 14, 28, and 29 constitute the vector-wedge method.

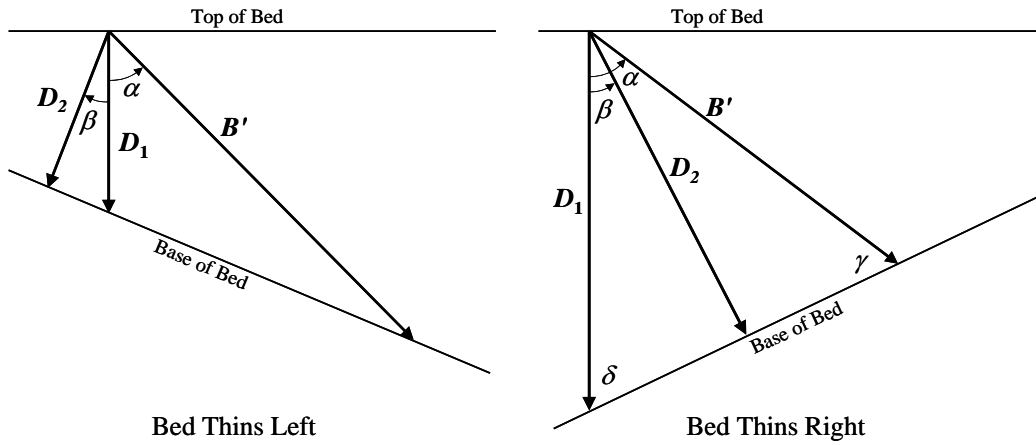


Figure 8. When the bed thins left, β and α are opposite directions from each other, but when the bed thins right, they are measured the same direction. This fact provides the sign for β in equation 28.

Calculation of TVT in the wedge-vector method is much simpler than for the fold-vector method, because it involves the intersection of the vertical TVT line with the plane of the dip at the base of the bed. Figure 9 shows the relationship of TVT to TST in the wedge-vector model.

The vector-component equation for the plane of the lower bed is

$$D_{2x}(x - D_{1x}TST) + D_{2y}(y - D_{1y}TST) + D_{2z}(z - D_{1z}TST) = 0. \quad (33)$$

Since the coordinates of a vertical line are $(0, 0, TVT)$, substitute these x , y , and z values into equation 33, solve for TVT and get

$$TVT = \frac{TST}{D_{2z}} D_1 \cdot D_2 \quad (34)$$

for finding TVT . Note that positive TVT is used in the vertical line coordinates to make the answer come out positive. To be consistent, TVT should bear the same sign as TST .

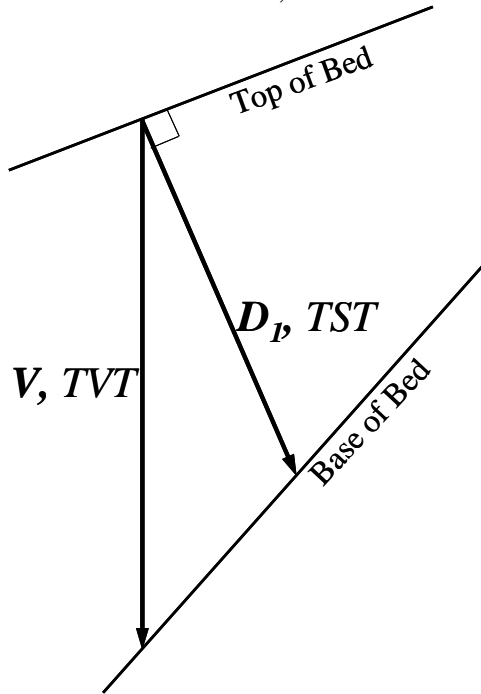


Figure 9. The relationship of TVT to TST in the wedge-vector model. Initially it would appear that TVT can be calculated by dividing the TST by the cosine of the dip of the base of the bed, but this is not true because this figure is in a vertical plane formed by the vectors V and D_1 , and thus has the azimuth of the top dip. Therefore, the dip at the base of the bed in this figure is an apparent dip.

DISCUSSION

Considerations in the Calculation of TST

Convergence with the Single-Dip Methods

As the upper and lower dips approach each other, the results of the fold-vector and wedge-vector methods approach the results single dip equations as they should.

However, if the dips are equal or the angle β is close to zero, then a single dip solution should be used to prevent calculation problems such as division by zero.

The Sign of TST

In some applications, the sign of TST is not important and can be ignored. However, in other applications, a negative sign is important because indicates that the borehole is traveling up section (Figure 10). The Setchell equation (1), the vectoral single-dip equation (5), and the average vector equation will automatically calculate the correct sign. In essence, what controls the sign of TST is the angle between the borehole and the dip pole. If the angle is less than 90° , then the angle is positive and if the angle is greater than 90° , then the angle is negative. An independent means of defining the sign of TST for these methods would be to multiply the absolute value of the number times the dot product of the vectors divided by absolute value of the dot product:

$$TST = |TST| \frac{\hat{\mathbf{D}} \cdot \hat{\mathbf{B}}}{|\hat{\mathbf{D}} \cdot \hat{\mathbf{B}}|}. \quad (35)$$

The fold-vector equation (11) will always calculate a positive result for TST . On the other hand, the wedge-vector equation will give both positive and negative results for TST , but not always consistent with the configuration of the dip vectors relative to the borehole vector. Offhand, one might think that the best way would be to use a vector mean of the two dip poles. In other words, use equation 35 with $\hat{\mathbf{D}}$ calculated from equation 8. On the other hand, the sign could possibly be calculated using $\hat{\mathbf{D}}_1$ in equation 35.

The cumulative error tests helped to determine the best way to calculate sign of TST for the fold-vector and wedge-vector models (see Appendix). For the fold-vector method, it was found that using $\hat{\mathbf{D}}$ was considerably more accurate, especially when the borehole was traveling roughly parallel to dip (such as in a horizontal well). For the wedge-vector method, using vector $\hat{\mathbf{D}}_1$ was noticeably more accurate overall, but not overwhelmingly so.

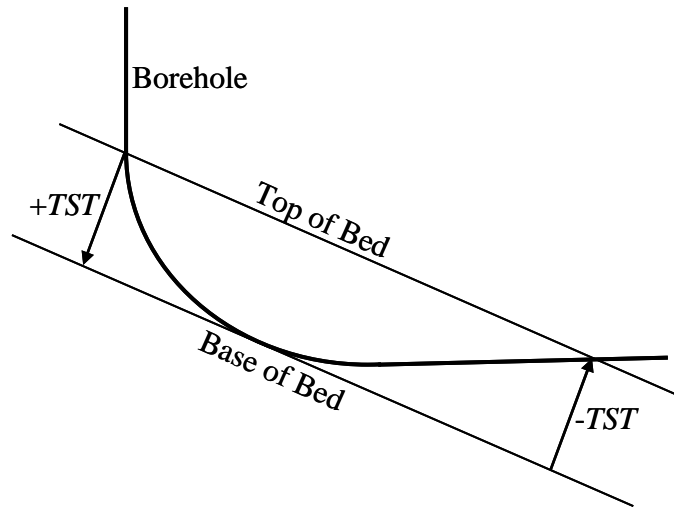


Figure 10. The reversal of *TST* sign. By convention, as the borehole is traveling down section, as as on the left, the sign is positive. When the borehole is traveling up section, as on the right, the sign of *TST* should become negative.

To be used in cumulative calculations, any method for determining *TST* should be reversible, that is, a borehole traveling the opposite direction through the same dips should come up with the same answer, only with reversed sign. This is true for the average-vector and fold-vector methods, but not for the wedge-vector method. In the wedge-vector method, when the borehole is traveling up section, the calculated *TST* will be different from the same configuration when traveling down section. Reversibility in such a case can be forced, however, by reversing the deviation direction, swapping the dips, and then making the sign of the result negative. In the cumulative error test, making the wedge vector model reversible improved the maximum cumulative error by about 0.5% over the non-reversed solution when the dips had random scatter of 10° (see Appendix).

The Accuracy of the Methods

Initially, fold-vector and wedge-vector methods were tested for correctness by checking with simple graphical examples. However, when the dip azimuths are different and the borehole has yet another azimuth, graphical checking becomes difficult. The

folded-bed and wedging-bed models of Xu, et al. (2007) and Xu, et al. (2010), respectively, were adapted to use two azimuths in order to double-check the fold-vector and wedge-vector models. (See Appendix for details.) Alternate derivations were used to check the *TVT* calculations as well.

Choosing a Calculation Method

Dips at Short Intervals

When formation imager dips or dipmeter dips are available, *TST* and *TVT* are commonly calculated as cumulative depths in log form. Such dips will be fairly close together and will have scatter caused by measurement error as well as natural variation. Initially, one might suspect that if any model were to be used, it would be the wedge-vector model since folds are not likely to be common in such a small scale, and it is common for smaller-scale sedimentary features to have significant thickening or thinning (wedging). It is not clear offhand, however, what the cumulative effect of both measurement error and natural scatter might be. In order to test the methods, random scatter was generated in a long interval with varying borehole angles. It was found, surprisingly, that the fold-vector method had by far the least cumulative error of the three, so it is the best method to use for short-interval dips (See Appendix for testing details). Remember that for dips with short intervals, sign is important for keeping track of relative stratigraphic position within a section.

Dips at Long Intervals

When log-measured dips are not available or they do not cover an entire interval, dips derived from subsurface or geophysical mapping may be used to calculate *TST*. This is where the geometry of the models is most important. In general, major stratigraphic units will have little thickness change within the lateral reach of a well, even when the well has traversed thousands of meters laterally. In most cases, the maximum change on dip caused by stratigraphic changes should be on the order of 1 or 2°. In fact, those dip magnitudes are probably within the error of measurement of dip data. Therefore, caution

should be used when applying the wedge-vector model. On the other hand, structural differences in dip can be much larger, making the fold-vector model the appropriate choice in most cases.

Xu, et al. (2010) propose mixing fold and wedge models. In the mixing scheme, they use linear averaging of the models. Although this seems a reasonable means of solving the problem, it is not known how accurate it might be because of the nonlinearity of the models. A better approach to combining the models would be to break up an interval proportionately to the relative amounts of folding and wedging. An intermediate dip would have to be interpolated (see interpolation section below) at the dividing point before calculating the respective *TST* values. The relative contributions of folding versus wedging in the interval could be determined on the basis of structural and isopach maps.

Interpolation

When doing *TST* calculations, every dip should have a deviation. The correct way to interpolate deviations is to interpolate the depths and coordinates from a deviation survey using the minimum curvature method of Taylor and Mason (1972). Another mathematical approach to interpolate deviation is to use Euler-pole rotation (Cox and Hart, 1986). As in deviation interpolation, efforts to interpolate between dips by interpolating the dips and azimuths separately can introduce error. Minimum curvature and Euler pole rotation can be adapted for dips as well.

Calculated dips derived from both formation image logs and from dipmeters are frequently accompanied by deviation data interpolated for each dip. Service companies will sometimes interpolate the inclinations and deviation azimuths separately. This is not the correct way to interpolate deviations. An example of how much error can be created by interpolating or averaging inclinations and azimuths separately would be to take two deviation measurements, the first having inclination of 1° and deviation azimuth due East. The second deviation has the same inclination, but deviation azimuth pointing due west. Averaging inclinations and azimuths separately yields 1° due South, when the true

answer should be 0° inclination. The angular error is 1° , which may not sound large, but it is the same magnitude of the input inclinations. In other words, separately interpolating inclination and azimuth needlessly adds to calculation error. Since the interpolations have to be done for most dips, the cumulative effect over a given interval can be large.

Another common error in angular interpolation is to interpolate the direction vectors by separately interpolating the direction cosines. This will always come up with the wrong answer except when the angle to be interpolated is exactly halfway between the starting and ending angle. (This fact is used in the average-vector derivation.) Again, the best way to interpolate between angles is either by the minimum curvature or Euler-pole rotation methods.

Averaging Dips before Calculation

When trying to refine dip data for *TST* calculation, averaging techniques may be used. There is a problem in averaging dips that occurs when operations are done on dip directions instead of dip poles. The problem is likely caused by the fact that a vector of the dip direction does not uniquely represent the dip plane. An example of this would be to take two dips, one 5° due East and one 5° due West. An average vector of the poles to dip (the vector mean) comes out with a correct dip of 0° . However, an average vector of the dips produces a vertical dip!

When averaging steep dips, care should be taken to decide when dips are overturned. Overturned dips can be represented numerically by subtracting the dip from 180° and changing the azimuth by 180° --in other words putting the pole in the opposite hemisphere. If this is not done, then the vector average will be wrong by a considerable amount. Alternatively, one can use eigenvector analysis (Woodcock, 1977, and Scheidegger, 1965) and use the major pole for the average dip. Eigenvector analysis is bidirectional, so whether or not a dip is overturned, the correct answer will be obtained. Because of the problem with overturned dips, it is generally believed that eigenvector analysis should usually be used when overturned dips are present but not defined

explicitly as such. If the overturned dips are defined, however, simple averaging (vector mean) can be used.

Calculation Pitfalls

When doing large numbers of any kind of calculation on a computer, it is common that an occasional problem, such as numeric overflow, will stop calculations entirely. The most commonly encountered problem encountered while testing the methods was an illegal arccosine of a number slightly greater than 1. This was caused by truncation errors generated when finding the magnitude of vectors. The problems were avoided by simply replacing those numbers whose magnitudes were very slightly greater than 1 with 1 within the arccosine function. Another common calculation problem is division by zero. In many cases, division by zero results from using too complicated a solution for the problem at hand. A good example of this would be where the top and bottom beds have the same dip when using the fold-vector equation. The solution, naturally, is to check for the condition and use the simpler relationship, for example, the Setchell or vectoral single-dip equations, for the fold vector problem above.

Another type of calculation problem results when there is no solution to the problem at hand. A good example is when calculating *TVT* for the fold-vector method. There are cases where an error, caused by taking the square root of a negative number, will result when the vertical line representing *TVT* does not intersect with the cylinder representing the base of the bed. In these cases, the result is legitimate and a way of displaying that fact must be implemented before the negative square root is attempted.

CONCLUSIONS

Three new two-dip methods of calculating *TST* and *TVT* have been introduced. They have been shown to be robust and accurate. It has also been demonstrated how to accommodate borehole curvature into the calculations.

Best practices have been suggested as to averaging and interpolation of dip and borehole deviation data. Averaging and interpolation are important because they are used both in the calculation of *TST* and *TVT* and the preparation of data for the calculations.

REFERENCES

- Bateman, R.M., and V.R. Hepp, 1981, Application of True Vertical Depth, True Stratigraphic Thickness[,] and True Vertical Thickness Log Displays, SPWLA Twenty-Second Annual Logging Symposium Transactions paper YY.
- Cox, Allan, and R. B. Hart, 1986, Plate tectonics; how it works: Boston, Blackwell Scientific Publications.
- Holt, O.R., L.G. Schoonover, and P.A. Wichmann, 1981, True Vertical Depth, True Vertical Thickness, and True Stratigraphic Thickness Logs, SPWLA Eighteenth Annual Logging Symposium Transactions paper Y.
- Marshak, S., and G. Mitra, 1988, Basic Methods of Structural Geology, Prentice-Hall, Inc., Englewood Cliffs, New Jersey.
- Parks, J. M., 1970, Computerized Trigonometric Method for the Rotation of Structurally Tilted Sedimentary Directional Features: GSA Bulletin, v. 81, p. 537-540.
- Taylor, H.L., and C.M. Mason, 1972, A Systematic Approach to Well Surveying Calculations, Society of Petroleum Engineers Journal, p474-488, Paper Number 3362-PA.
- Tearpock, D.J., and R.E. Bischke, 1991, Applied Surface Geological Mapping, Prentice-Hall, Inc. Englewood Cliffs, New Jersey.
- Scheidegger, A. E., 1965, The tectonic stress and tectonic motion direction in Europe and western Asia as calculated from earthquake fault plane solutions: Seismol. Soc. America Bull., v. 54, p. 1519-1528.
- Weisstein, E. W., 2012, "Point-Line Distance--3-Dimensional." From MathWorld--A Wolfram Web Resource, URL--<http://mathworld.wolfram.com/Point-LineDistance3-Dimensional.html>.
- Woodcock, N. H., 1977, Specification of fabric shapes using an eigenvalue method: Geol. Soc. America Bull., v. 88, p. 1231-1236.

Xu, S-S, L.G. Velasquillo-Martínez, J. M. Grajales Nishimura, G. Murillo-Muñetón, J. G. Hernández, and A. F. Nieto-Samaniego, 2007, Determination of True Bed Thickness Using Folded Bed Model and Borehole Data, *Journal of Canadian Petroleum Technology*, Vol. 46, No. 11, p.15-20.

Xu, S-S., A.F. Nieto-Samaniego, J. M. Grajales Nishimura, L.G.Velasquillo-Martínez, G. Murillo-Muñetón, J. García-Hernández, 2010, A folded wedge model for determination of true stratigraphic thickness in directional wells, *Int. J. Oil, Gas and Coal Technology*, Vol. 3, No. 3, p.245–268.

APPENDIX

Deriving the Setchell Equation from the Single-Dip Vectoral Equation

The Setchell equation (1) can be derived from the vectoral equation 4 by substituting the spherical to rectangular conversions below:

$$\hat{D}_x = \sin \varphi \sin(\theta_d - \pi), \quad (\text{A-1})$$

$$\hat{D}_y = \sin \varphi \cos(\theta_d - \pi), \quad (\text{A-2})$$

$$\hat{D}_z = -\cos \varphi, \quad (\text{A-3})$$

$$\hat{B}_x = \sin \psi \sin \theta_b, \quad (\text{A-4})$$

$$\hat{B}_y = \sin \psi \cos \theta_b, \text{ and} \quad (\text{A-5})$$

$$\hat{B}_z = -\cos \psi, \quad (\text{A-6})$$

where \hat{D} is the dip-pole vector and \hat{B} is the borehole vector. In this geographic coordinate system, positive x is east, positive y is north, and positive z is upward. This coordinate system is standard for geological mapping. Note that the dip poles are in the lower hemisphere. This makes the sign of calculated TST positive when drilling down section (from top to bottom), which follows convention. Note also that this coordinate system conflicts with the convention for deviation calculation, which has z positive downward.

Expressing the vectoral equation 4 in terms of direction cosines yields

$$TST = MT \left(\hat{D}_x \hat{B}_x + \hat{D}_y \hat{B}_y + \hat{D}_z \hat{B}_z \right). \quad (\text{A-7})$$

Substituting equations A-1 through A-6 into equation A-7 and simplifying results in the Setchell equation (1) repeated below:

$$TST = MT \left(\cos \psi - \sin \psi \cos(\theta_d - \theta_b) \tan \varphi \right) \cos \varphi. \quad (\text{A-8})$$

This means that the Setchell equation is equivalent to the vectoral single-dip equation (5). There are simpler derivations possible—this derivation demonstrates the equivalence of the Setchell and vectoral equations.

Projecting the Borehole onto the Two-Dip Plane

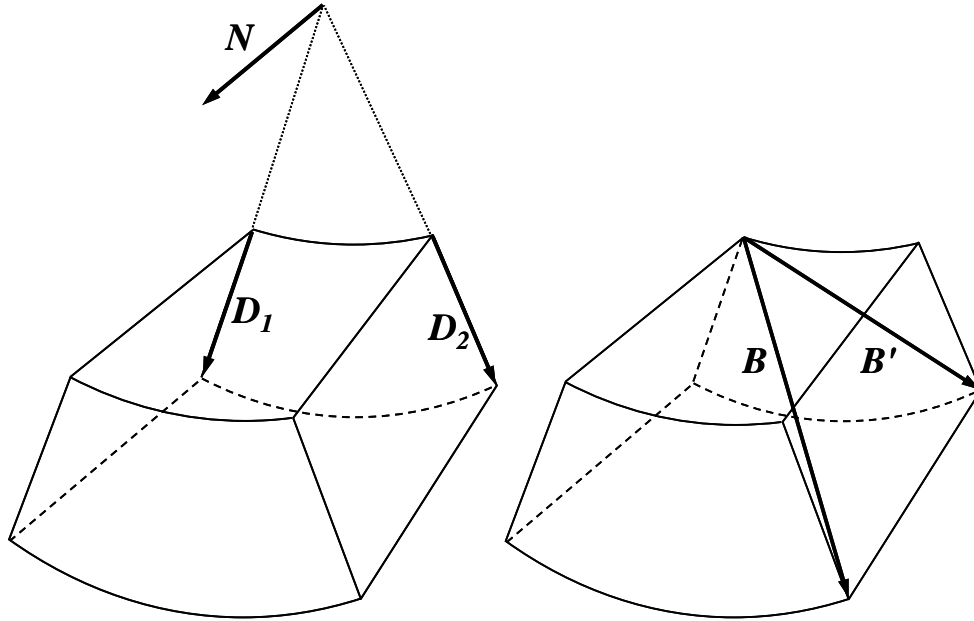


Figure A-1. How the borehole vector B is projected along the fold axis of a concentric fold to get the borehole projection B' . Left: The axis vector N is calculated as the cross product of vectors \hat{D}_1 and \hat{D}_2 . Right: The borehole vector B is projected parallel to the axis to calculate B' .

Figure A-1 shows the configuration between vectors B , B' , and the fold. Vector B' is the projection of the borehole vector B onto the plane in which the dip vectors \hat{D}_1 and \hat{D}_2 lie. Projecting a vector that starts at the origin onto a plane that goes through the origin is fairly straightforward. A plane can be represented by a normal to the plane. Taking the cross product will get the normal

$$\hat{N} = \frac{\hat{D}_1 \times \hat{D}_2}{|\hat{D}_1 \times \hat{D}_2|}, \quad (\text{A-9})$$

where \hat{N} is the normal to the two dip vectors. To get the projection of the borehole vector onto the plane, first we make a vector whose direction is defined by \hat{N} and whose length is defined by the distance of B from the plane. Then that vector is subtracted from vector B :

$$\mathbf{B}' = \mathbf{B} - \hat{\mathbf{N}} \cdot p, \quad (\text{A-10})$$

where p is the distance of the point of the vector from the plane. The distance p is found by the relationship

$$p = \hat{\mathbf{N}} \cdot \mathbf{B}, \quad (\text{A-11})$$

Substituting equation 11 into equation 10 we get

$$\mathbf{B}' = \mathbf{B} - \hat{\mathbf{N}} (\hat{\mathbf{N}} \cdot \mathbf{B}), \quad (\text{A-12})$$

the equation for the projection of the borehole onto the plane containing the two dip normals.

Fold-vector *TVT* Derivation

In this derivation, *TVT* is the length of the vertical vector \mathbf{V} that starts where the borehole intersects the top of the bed and ends where \mathbf{V} touches the base of the bed (Figure A-2). The basic problem is to find the point of intersection of \mathbf{V} with the cylinder of the bed base.

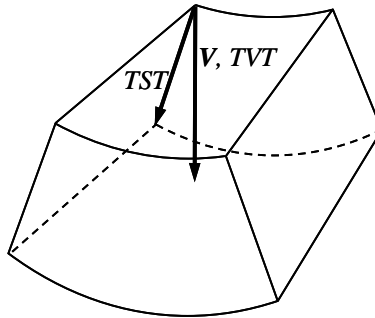


Figure A-2. The configuration for derivation of the *TVT* equations for the fold-vector model. *TVT* is the length of a vertical vector \mathbf{V} that starts where the borehole intercepts the top of the bed and ends at the base of the bed.

To set up the derivation, we must first define the cylindrical surface that will be intersected by the vertical vector \mathbf{V} . A cylinder can be represented vectorally as a shape whose points are equally distant from a given line. Weisstein (2012) gives the following vectoral formula for the distance of a point to a line:

$$d = \frac{|(\mathbf{x}_2 - \mathbf{x}_1) \times (\mathbf{x}_1 - \mathbf{x}_0)|}{|\mathbf{x}_2 - \mathbf{x}_1|}, \quad (\text{A-13})$$

where d is the distance, \mathbf{x}_1 and \mathbf{x}_2 are points on the line, and \mathbf{x}_0 is a point that is d distance from the line.

The distance in equation A-13 is the radius R of the base-bed cylinder. Since we are in a plane perpendicular to the cylinder, the cylinder can be treated as a circular section. The general equation for a chord of a circle is

$$C = 2R \sin\left(\frac{\beta}{2}\right), \quad (\text{A-14})$$

where C is the length of the chord. From Figure 6, using the law of sines yields

$$C = TST \frac{\sin \alpha}{\sin \gamma}. \quad (\text{A-15})$$

Combining equations 14 and 15 and solving for R gives

$$R = \frac{TST \sin \alpha}{2 \sin \gamma \sin\left(\frac{\beta}{2}\right)}. \quad (\text{A-16})$$

The line will be the axis of the fold and the base surface of the bed will be the cylinder whose points are equidistant from the axis. As mentioned in the *TST* derivation, there are two possible configurations, the concave upward and the concave downward (Figure A-3). The vector \mathbf{E} spans the shortest distance of the axis to the origin. The vector equation for \mathbf{E} for the concave-upward case is

$$\mathbf{E} = \mathbf{D}_1(R - TST). \quad (\text{A-17})$$

and the equation for the convex-upward case is

$$\mathbf{E} = -\mathbf{D}_1(R + TST), \quad (\text{A-18})$$

Equation A-19 can be rewritten as

$$\mathbf{E} = \mathbf{D}_1(-R - TST). \quad (\text{A-19})$$

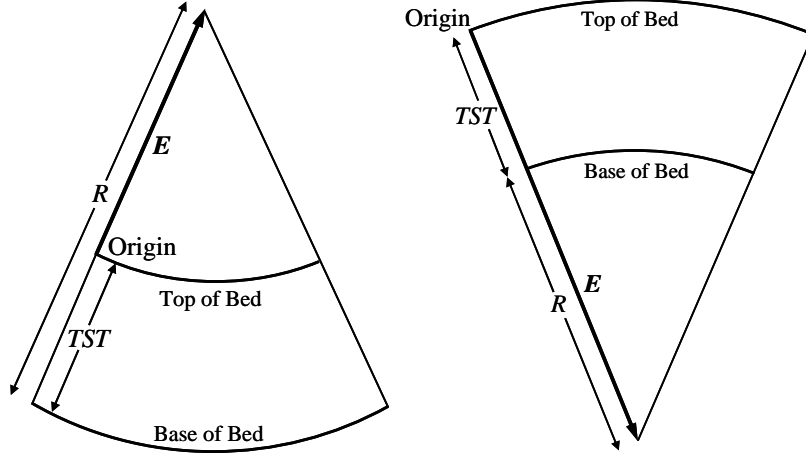


Figure A-3. The concave-upward case (left) and the convex-upward case (right) showing the relationships of the E vector to R and TST . The terms “anticline” and “syncline” do not necessarily apply, because this figure lies in an arbitrary, non-vertical plane. The E vector, which starts at the origin, will define the point at the apex of the base-of-bed sector. Its length will be the distance of the cylindrical axis from the origin. In the concave-upward case, the length of E is $R - TST$, while in the convex-upward case, the length of E is $R + TST$.

The concave-upward and convex-downward cases can be determined in exactly the same way as the left-thinning and right-thinning cases of the wedge-vector model using equation 31. Concave-upward is equivalent to right thinning and convex-upward is equivalent to left-thinning. Combining equation 31 with equations A-17 and A-19 yields

$$\mathbf{E} = D_1 (s \cdot R - TST). \quad (20)$$

In equation 13, vector E can serve as the distance vector of the line from the origin, \mathbf{x}_0 , and it can also serve as a point on the cylindrical axis, \mathbf{x}_1 . To define the other point on the cylindrical axis (\mathbf{x}_2), the normal to the dip plane, \hat{N} (from equation 9), can be added to E . Substitution of these relationships and R for d into equation 13 yields

$$R = \frac{\left| \left((\hat{N} + E) - E \right) \times (E - V) \right|}{\left| (\hat{N} + E) - E \right|} \quad (A-21)$$

Since a vertical vector starting at the origin will have its x and y components equal to 0,

$$\mathbf{V} = (0, 0, -TVT). \quad (\text{A-22})$$

Inserting the vector components in A-22 into equation A-21 and simplifying yields

$$A \cdot TVT^2 + 2B \cdot TVT + C = 0, \quad (\text{A-23})$$

where

$$A = \hat{N}_x^2 + \hat{N}_y^2, \quad (\text{A-24})$$

$$B = \hat{N}_x G + \hat{N}_y H, \quad (\text{A-25})$$

$$C = F^2 + G^2 + H^2 - R^2, \quad (\text{A-26})$$

$$F = \hat{N}_x E_y - \hat{N}_y E_x, \quad (\text{A-27})$$

$$G = \hat{N}_x E_z - \hat{N}_z E_x, \text{ and} \quad (\text{A-28})$$

$$H = \hat{N}_y E_z - \hat{N}_z E_y. \quad (\text{A-29})$$

Solving equation A-23 for TVT yields

$$TVT = -\frac{B \pm \sqrt{B^2 - A \cdot C}}{A}, \quad (\text{A-30})$$

the fold-vector equation for TVT .

One more step needs to be done to find the correct answer. The “plus or minus” (\pm) symbol in equation A-30 indicates that there are two solutions for TVT . This is because a line has two possible intersections with a cylinder. In the concave-upward case, the origin is entirely within the cylinder, so the correct answer is the smallest value of TVT , since \mathbf{V} always points downward. In the convex-upward case, both intersections are below the origin, thus we need the shortest distance, or the smallest absolute value of TVT . After the right value for TVT is found, it should be given the same sign as TST .

Testing the Accuracy and Robustness of the Fold-Vector and Wedge-Vector Models

Three types of random tests were conducted on the models. The first test was a stress test that was done to make sure that a rotation of the entire system would not affect TST calculations. (TVT calculations, on the other hand, are affected by rotation because the vertical vector will change when the system is rotated.) Another type of stress test

was designed to test the accuracy and robustness of both the *TVT* and *TST* methods. The last type of test was the cumulative error test that was run only on the *TST* models. It tested over a more natural range of variation than the other tests in order to check the accuracy and internal consistency of the models.

In all except the cumulative error tests, poles and deviations were randomly generated over the maximum possible ranges. The dips and inclinations ranged from 0 to 180°, and azimuths ranged from 0 to 360°. Configurations were eliminated that were geometrically “impossible”, such as in the fold-vector model when the borehole would penetrate the top of the bed twice before hitting the base of the bed. Although the impossible configurations did not create problems for the *TST* calculations, they interfered with the logic of the *TVT* calculations.

The Rotation Test

In this test, calculations were performed twice for the fold-vector, average-vector, and wedge-vector methods. The first set of calculations was run with rotational dip of 0° and the second set was run with a randomly generated rotation dip. Out of 100,000 samples, there were a total of 28 disagreements between rotated and non-rotated calculations. All of the disagreements were with α , β , or γ equal to 90°, or β equal to 0°, and were related entirely to the math and not to any problem with the rotation itself. Unlike *TST*, *TVT* will change with rotation because the relative position of vertical line will change relative to the dips and deviations.

Testing the TST Models

A common property of geometrical derivations is that if they are derived for one configuration, a different configuration may get a different answer. A good example is the sign of β in the wedge-vector equation 28. In both the fold-vector and wedge-vector methods, multiple derivations were tried, each of which had its computational quirks. Since many of the cases are similar between the different derivations, comparing the different derivations to each other may not be the best way to cross check results.

Graphical solution may help in confirming results, but it is easy to overlook cases. To make sure all cases are covered properly, completely different methods of calculation were derived. Two analogues to the fold-vector and wedge-vector models exist, the folded-bed and wedging-bed models, respectively, from Xu, et al., 2007, and Xu et al., 2010. Although the configurations are similar to their counterparts derived here, there is a major difference in that both of the Xu, et al. models implicitly assume that the two dips have the same azimuth. In their derivations, the borehole was projected onto the vertical dip-azimuth plane using a trigonometric relationship. The strength of this type of derivation is that the relative orientations are all well constrained, as opposed to the vectoral derivations here where everything is projected onto a plane in which the relative orientations of the components is easily visualized. Of course, the main problem with a vertical-plane derivation is just that—it assumes a single azimuth. The adaptation of these models to separate dip azimuths was accomplished by rotating the two-dip and borehole system until the first dip is zero. Since the relative positions remain the same, the *TST* cannot change. The rotation method used is essentially the same as for the removal of structural tilt (See Parks, 1970). The rotated first dip is zero and can have any azimuth; therefore the two-azimuth system resolves into a single azimuth, that of the rotated second dip, and the rotated values can be plugged into the folded-bed and wedging-bed equations. The modified folded-bed and wedging-bed models also verified the borehole projection equation 9, because they used an entirely different means to project the borehole onto the plane of section.

In 100,000 tests, there were approximately 20 disagreements between the fold-vector and modified folded-wedge models and about the same number between the wedge-vector model and the modified wedging-bed models. All of the mismatches were caused either when the angle between the borehole and the first dip pole was equal to 90° or when the angle between the two dip poles was equal to either 90° or 180° . These are special circumstances not likely to be encountered very often with actual data. That

being said, it appeared that the fold-vector model consistently had the same answers when the calculation precision changed, while the modified folded-bed model was not always consistent with itself as the precision changed. It is likely, therefore, that the fold-vector model is slightly more accurate. On the other hand, most of the mismatches between the wedge-vector and modified wedging-bed models usually happened when the calculated *TST* values were very large. In the testing above, the random angles generated were integers. When the random numbers generated had 4 decimal places, there were no mismatches, even with 1,000,000 tests. This simply means is that integers were more likely to randomly generate the 90° or 180° exceptions.

Testing the TVT Models

Fold-Vector TVT

As mentioned before, geometrical derivations have the tendency to change with different configurations. With that in mind, an alternate means of calculating *TVT* was derived based on the intersection of a line with a circle. The 3D cylinder-line intersection was reduced to a 2D circle-line intersection in the *y-z* plane by rotating the system until vector D_1 was vertical. In 1,000,000 random tests, there were 32 disagreements between the two methods, all of which were between two very large numbers (on the order of $\pm 10^{20}$) or between a very large number and no answer (no intersection of the line with the cylinder). Although alarming, the very large numbers are extremely unlikely to be encountered with actual data.

Wedge-Vector TVT

The vectoral method for calculating wedge-vector *TVT* was tested against two alternative, geometric derivations. One derivation was in the vertical plane with the first dip pole and had the second dip represented as an apparent dip. The other derivation was similar to the circle-line derivation for fold-vector *TVT*, except that the 2D line intersected another 2D line instead of a circle. There were many more disagreements between the three methods, approximately 5,600 out of 100,000 randomly generated

problems. This is because wedge-vector *TST* itself gets very large in some instances as mentioned above. As in the fold-vector *TVT* calculations, nearly all the disagreements were between very large numbers on the order of $\pm 10^{20}$. There were a few disagreements between methods with reasonably-sized answers, but these were always when the difference between the two dips was exactly 90° or the differences between the two dip azimuths were exactly 180° . Bear in mind that the problems were generated randomly, and that, in nature, it would be rare in stratigraphic wedging to have the dip difference exceed 20° , and a dip difference greater than about 45° is virtually impossible because of the maximum angle of repose.

Testing Cumulative Error for TST

Dip data from logs can have significant scatter. The scatter can be caused either by measurement error or natural variation. In order to test the sensitivity of the various models to scatter, hypothetical logs were generated with the assumption of constant dip through an entire interval, but with random scatter added in (Figure A-3). The summed *TST* values were compared with the value that an entire interval would have had at constant dip. This was done with scatter of 5° and 10° with borehole angle relative to dip calculated at 5° increments from 0° to 180° . At each of the borehole angles there were 100,000 calculations per model.

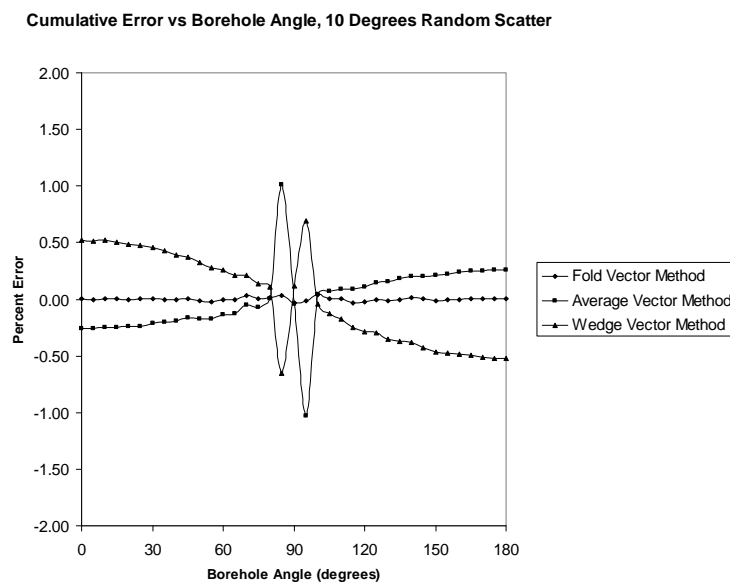
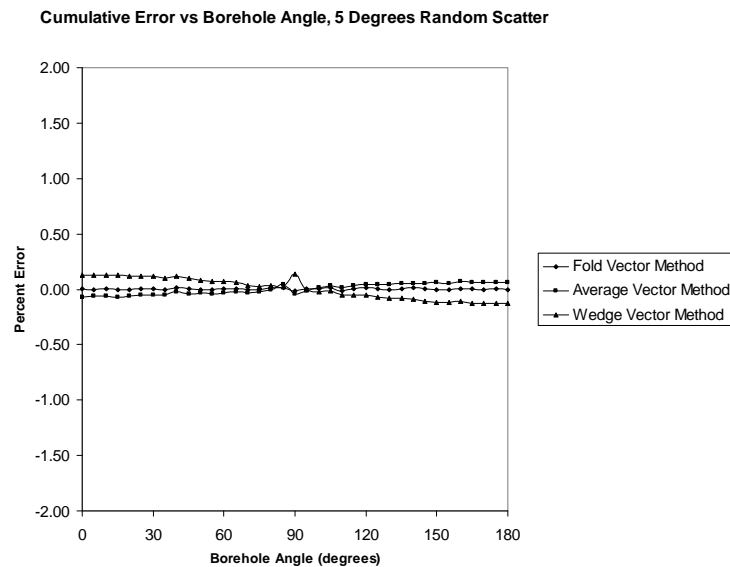


Figure A-1. Cumulative error with 5° and 10° scatter over a range of relative borehole angles to dip normals. (0° borehole angle would be equivalent to a vertical well in horizontal dips and 90° borehole angle would be equivalent to a horizontal well in horizontal dips.) Each point on each plot represents 100,000 calculations. In all cases, the fold-vector model had the smallest error.

Although the fold-vector model had the lowest error, at no point did any method exceed about 1% error over the entire interval. As mentioned before, removing the reversibility of the wedge-vector method increased the maximum error by about 0.5%-- not a lot, but confirming that forcing reversibility is justified.

These scatter tests are more severe than they might seem, because the distribution is not lognormal but constant throughout the interval, and also because the actual scatter is effectively double the number used. (Since the two equal dip magnitudes with opposite azimuths will have an angular difference of twice the dip magnitude.) Thus it would appear that all of these methods should be adequate for log or imager derived dips. It should be noted, though, that the wedge-vector method can reach very large numbers when the angle between the dips approaches 90° . This is not likely to happen very often, but if it does it is likely to cause severe problems. In other words, do not use the wedge-vector method if the data have a lot of scatter or, for example, if there is the chance that fractures have been mislabeled as beds. (This could easily happen with dipmeter-derived data in which type of dip is unknown.)